Electronic Supplementary Material (ESI) for Journal of Materials Chemistry A.

SUPPORTING INFORMATION

Operando X-Ray Absorption Investigations into the Role of Fe in the Oxygen Evolution Activity and Stability of $Ni_{1-x}Fe_xO_y$ Nanoparticles

Daniel F. Abbott[a], Emiliana Fabbri[a], Mario Borlaf[b], Francesco Bozza[b], Robin Schäublin[c], Maarten Nachtegaal[d], Thomas Graule[b], Thomas J. Schmidt[a,e]*

[a]*Electrochemistry Laboratory, Paul Scherrer Institut, CH-5232 Villigen PSI, Switzerland*
[b]*Laboratory for High Performance Ceramics, Empa, Swiss Federal Laboratories for Materials Testing and Research, 8600 Dübendorf, Switzerland*
[c]*Scientific Center for Optical and Electron Microscopy, Department of Chemistry and Applied Biosciences, ETH Zürich, CH-8093 Zürich, Switzerland*
[d]*Paul Scherrer Institut, CH-5232 Villigen PSI, Switzerland*
[e]*Laboratory of Physical Chemistry, ETH Zürich, CH-8093 Zürich, Switzerland*
**Email - daniel.abbott@psi.ch*

Table S1. Calculated atomic Fe and Ni compositions for the $Ni_{1-x}Fe_xO_y$ samples based on ICP and EDX analysis of the dry sample powders.

Sample	ICP Analysis		EDX Analysis	
	Fe, at.%	Ni, at.%	Fe, at.%	Ni, at.%
NiO	0.01	99.99	-	-
$Ni_{90}Fe_{10}O_y$	9.93	90.07	11.34 ± 0.73	88.66 ± 0.73
$Ni_{70}Fe_{30}O_y$	30.09	69.91	16.83 ± 2.59	83.17± 2.59

EXAFS Analysis

Extended X−ray absorption fine structure (EXAFS) data were analyzed using the Demeter program package, which included energy calibration (based on the simultaneously measured Ni or Fe reference foil), background subtraction, and edge step normalization. The resulting spectra were converted to the photoelectron wave vector k (in units $Å^{-1}$) by assigning the photoelectron energy origin, E_0, corresponding to $k = 0$, to the first inflection point of the absorption edge. The resulting Ni $\chi(k)$ functions were weighted with k^2 to compensate for the dampening of the XAFS amplitude with increasing k. These $\chi(k)$ functions were Fourier transformed over 2.6−14.0 $Å^{-1}$ for the dry catalyst samples. The amplitude reduction factor, S_0^2, was calculated separately for each sample from the respective scattering paths using the ab initio FEFF 6.2 code and assuming the coordination numbers based on the NiO rock salt structure. This is a reasonable assumption given that all $Ni_{1-x}Fe_xO_y$ samples closely resemble bulk NiO as evidenced by the high degree of crystallinity observed in XRD (Figure 3) and the cubic crystallites seen in the TEM analysis (Figure 1). The same approach was also used for fitting the dry samples at the Fe K-edge. In this case, however, all Ni atoms in the FEFF input file were replaced by Fe in order to generate an appropriate fitting model. The Fe $\chi(k)$ functions were Fourier transformed over 3.0−11.5 $Å^{-1}$.

In order to directly compare all of the $Ni_{1-x}Fe_xO_y$ samples, a simple three−shell model based on the NiO rock salt structure was employed to fit the EXAFS data. A single Ni–O1 scattering path was used to describe the 6 nearest neighbor oxygen atoms (R_{eff} = 2.089 Å) in the first coordination shell. For fitting the second shell, a single Ni–Ni scattering path (R_{eff} = 2.954 Å) was used in addition to a second Ni–O2 scattering path (R_{eff} = 3.618 Å). The inclusion of the additional Ni–O scattering path was required in order to capture all of the signal as can be seen by the best fit of χ(Im) and χ(qre) (Figure S1, S4-6).

The same EXAFS fitting approach used for the dry catalyst samples was also used for the *operando* EXAFS data. In this case, however, S_0^2 was calculated separately for each sample while assuming the coordination numbers based on the NiO rock salt structure for the starting potential (i.e. 1.2 V). This is a reasonable assumption considering that we are close to the resting potential (i.e. open circuit potential, OCP) where we expect Ni to be fully coordinated ($N_{Ni–O}$ = 6). The calculated values for S_0^2 were then held constant and used in all subsequent FEFF calculations for each respective $Ni_{1-x}Fe_xO_y$ sample while the Ni–O1 coordination number, bond distance, and Debye-Waller factor parameters were allowed to vary. The Ni–Ni and Ni–O2 coordination numbers were also kept at constant values based on the NiO rock salt structure. The χ(*k*) functions were Fourier transformed over 2.6−12.5 $Å^{-1}$ for all *operando* data.

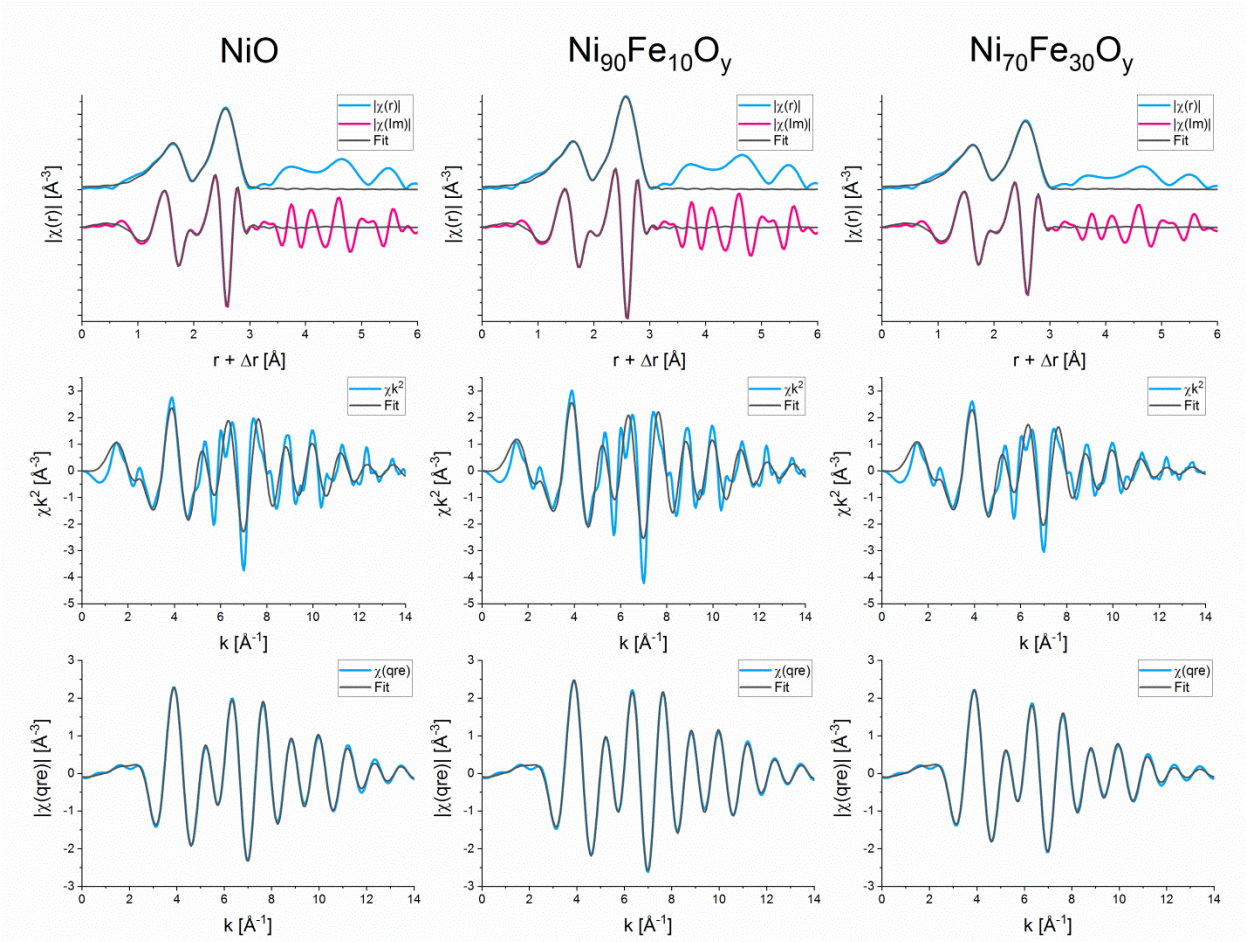

Figure S1. Fitted Fourier transformed Ni K-edge EXAFS spectra for the dry $Ni_{1-x}Fe_xO_y$ catalyst powders in r-space (top row), *k*-space (middle row), and *q*-space (bottom row). All Ni χ(*k*) functions were Fourier transformed over a k-range of 2.6 – 14.0 Å.

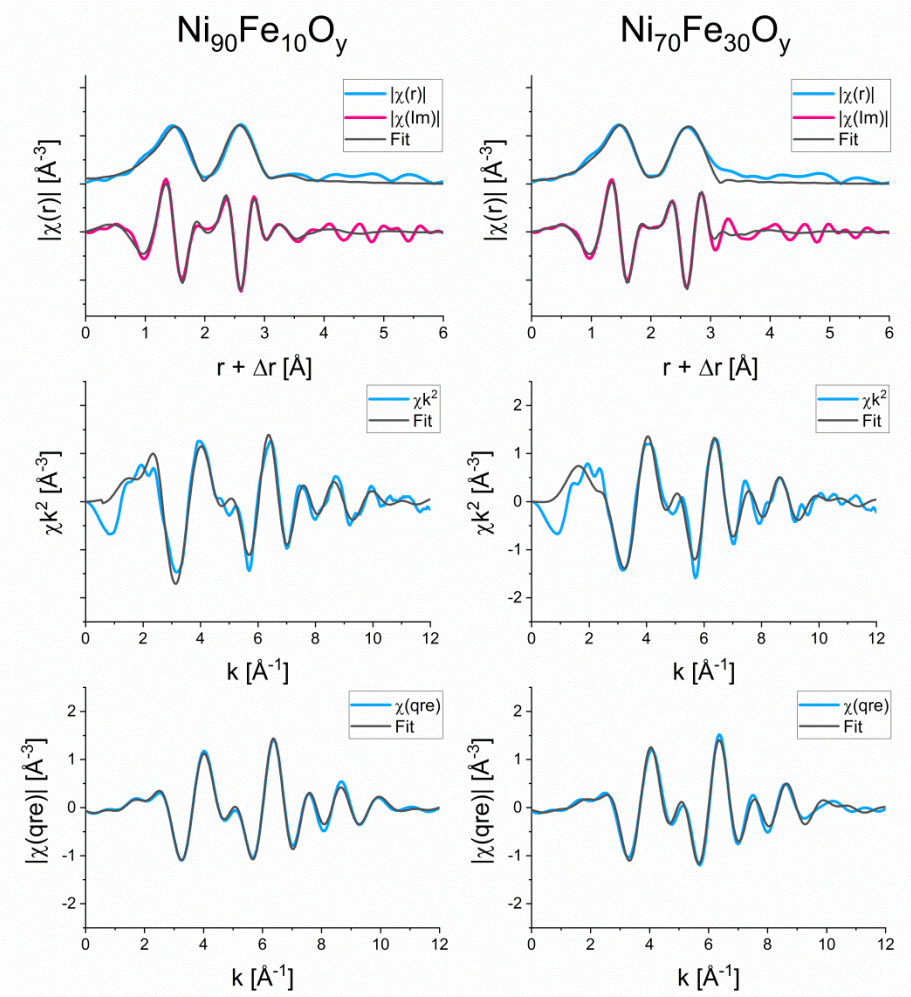

Figure S2. Fitted Fourier transformed Fe K-edge EXAFS spectra for the dry $Ni_{1-x}Fe_xO_y$ catalyst powders in r-space (top row), *k*-space (middle row), and *q*-space (bottom row). All Fe χ(*k*) functions were Fourier transformed over a k-range of 3.0 – 11.5 Å.

Table S2. Summary of the EXAFS best fit parameters for the dry $Ni_{1-x}Fe_xO_y$ catalyst powders at the Fe K-edge. *N* denotes the coordination number of the given scattering path, *d* indicates the refined path length, σ^2 represents the Debye-Waller factor, is ΔE_0 is the energy shift, S_0^2 is the amplitude reduction factor, and the R−factor represents the relative fit error of the fit.

Sample	Scattering Path	N	d, Å	σ^2, Å^2	$S0_2$	ΔE_0, eV	R-factor
$Ni_{90}Fe_{10}O_y$	Fe−O1	6	1.993 ± 0.010	0.0094 ± 0.0020	0.75 ± 0.09	1.37 ± 1.05	0.0119
	Fe−Fe	12	3.015 ± 0.011	0.0144 ± 0.0015			
	Fe−O2	8	3.828 ± 0.042	0.0168 ± 0.0082			
$Ni_{70}Fe_{30}O_y$	Fe−O1	6	1.962 ± 0.019	0.0081 ± 0.0036	0.70 ± 0.17	-2.19 ± 2.19	0.0298
	Fe−Fe	12	3.005 ± 0.019	0.0161 ± 0.0033			
	Fe−O2	8	3.348 ± 0.053	0.0074 ± 0.0077			

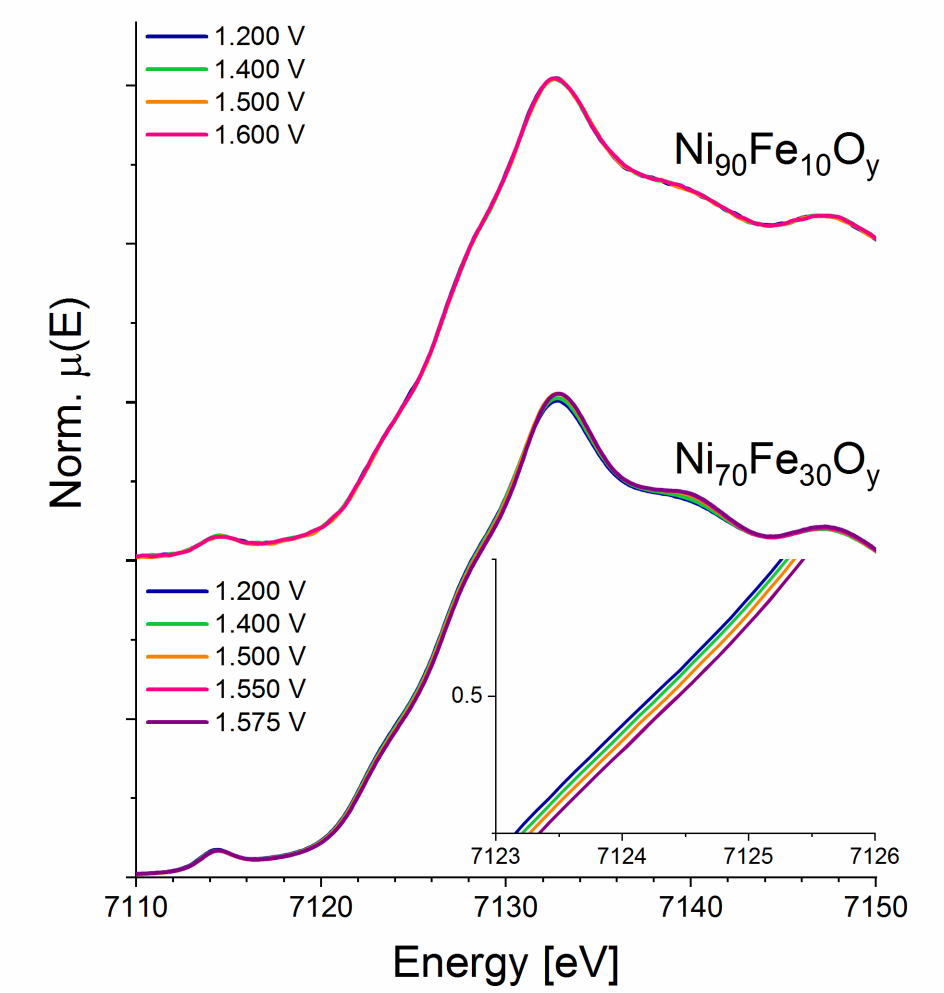

Figure S3. Normalized Fe K-edge XANES spectra recorded in *operando* for $Ni_{1-x}Fe_xO_y$ over a range of applied potentials. The inset shows an expansion of the absorption edge for $Ni_{70}Fe_{30}O_y$ to highlight the slight change in position.

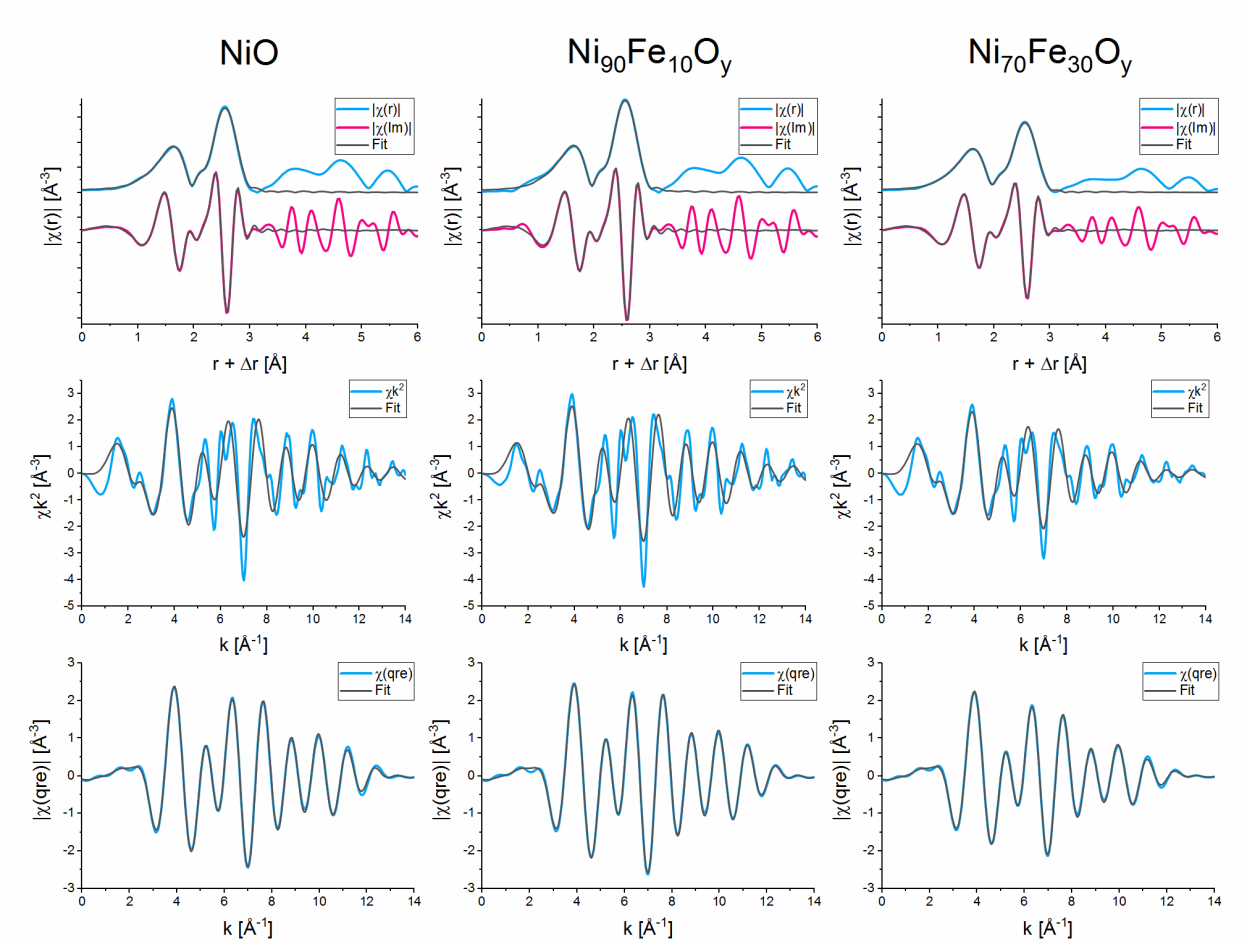

Figure S4. Typical examples of the fitted Fourier transformed Ni EXAFS spectra measured at 1.20 V during the *operando* OER polarization for $Ni_{1-x}Fe_xO_y$ in r-space (top row), *k*-space (middle row), and *q*-space (bottom row). All Ni χ(*k*) functions were Fourier transformed over a k-range of 2.6 – 12.5 Å.

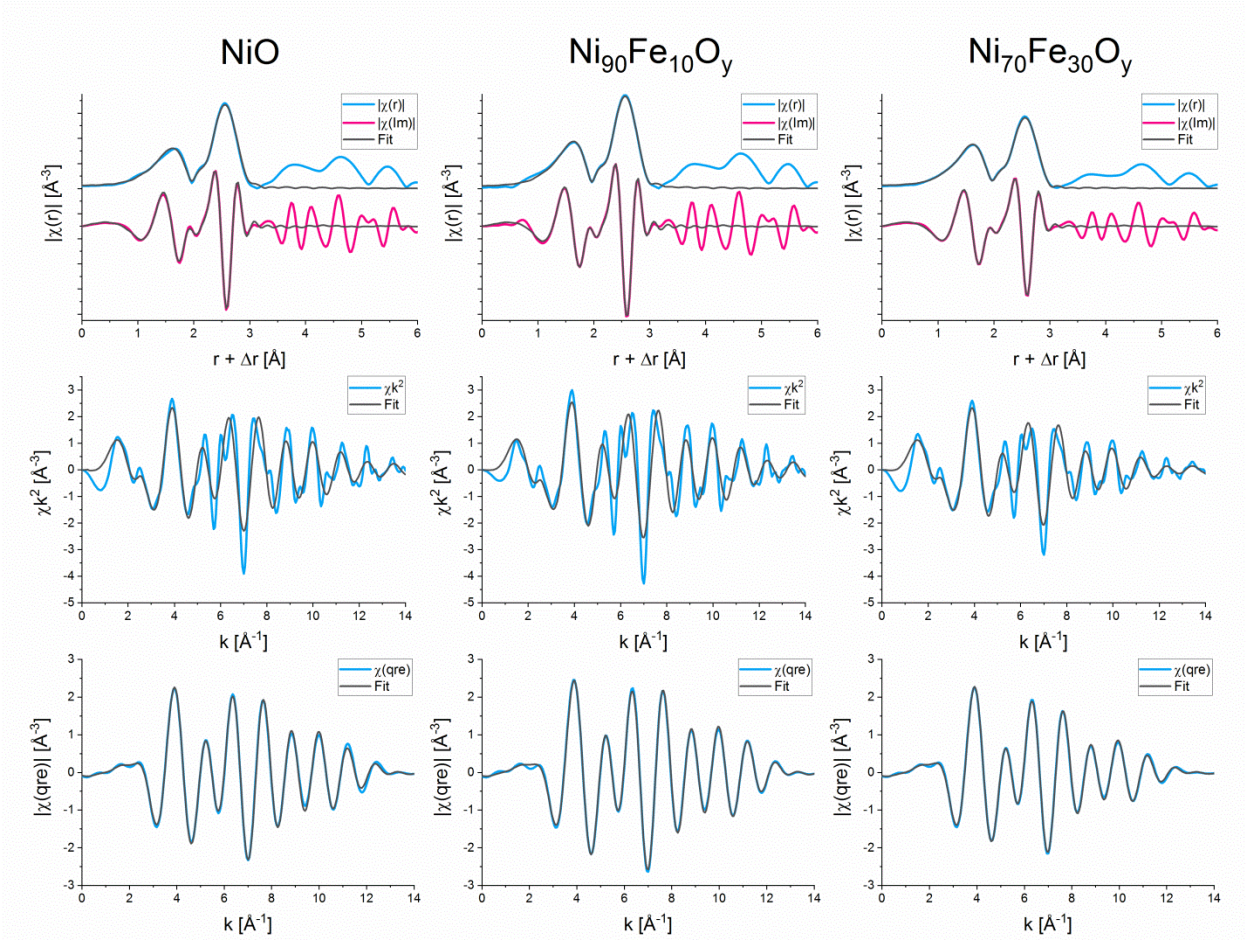

Figure S5. Typical examples of the fitted Fourier transformed Ni EXAFS spectra measured at 1.50 V during the *operando* OER polarization for $Ni_{1-x}Fe_xO_y$ in r-space (top row), *k*-space (middle row), and *q*-space (bottom row). All Ni χ(*k*) functions were Fourier transformed over a k-range of 2.6 – 12.5 Å.

Table S3. Summary of the EXAFS best fit parameters for the prepared NiO* sample recorded at different electrode potentials. *Operando* X−ray absorption spectra were measured at the Ni K edge during a standard electrochemical OER polarization measurement. *N* denotes the coordination number of the given scattering path, *d* indicates the refined path length, σ^2 represents the Debye-Waller factor, ΔE_0 is the energy shift, and the R-factor represents the relative error of the fit and data. An amplitude reduction factor of S_0^2 = 0.94 was used. *k* was kept within the range of *k* = 2.6−12.5 $Å^{-1}$ and a fitting window of 3.4 Å in R-space was used in all cases. C is used to indicate the potential steps recorded during the cathodic scan.

E, V	Scattering Path	N	d, Å	σ^2, $Å^2$	E_0, eV	R-factor
1.20	Ni−O1	6.0 ± 0.4	2.071 ± 0.006	0.0063 ± 0.0012	-0.18 ± 0.49	0.0038
	Ni−Ni	12	2.958 ± 0.004	0.0073 ± 0.0002		
	Ni−O2	8	3.535 ± 0.024	0.0121 ± 0.0031		
1.30	Ni−O1	5.9 ± 0.4	2.071 ± 0.006	0.0062 ± 0.0011	-0.19 ± 0.48	0.0036
	Ni−Ni	12	2.958 ± 0.004	0.0073 ± 0.0002		
	Ni−O2	8	3.536 ± 0.023	0.0122 ± 0.0031		
1.40	Ni−O1	5.9 ± 0.4	2.070 ± 0.006	0.0064 ± 0.0012	-0.13 ± 0.48	0.0037
	Ni−Ni	12	2.957 ± 0.004	0.0073 ± 0.0002		
	Ni−O2	8	3.535 ± 0.024	0.0124 ± 0.0031		
1.45	Ni−O1	5.8 ± 0.4	2.070 ± 0.007	0.0071 ± 0.0013	0.10 ± 0.50	0.0040
	Ni−Ni	12	2.956 ± 0.004	0.0073 ± 0.0002		
	Ni−O2	8	3.540 ± 0.025	0.0131 ± 0.0033		
1.50	Ni−O1	5.8 ± 0.5	2.070 ± 0.007	0.0077 ± 0.0015	0.25 ± 0.54	0.0047
	Ni−Ni	12	2.956 ± 0.004	0.0073 ± 0.0003		
	Ni−O2	8	3.542 ± 0.026	0.0135 ± 0.0035		
1.55	Ni−O1	5.6 ± 0.5	2.070 ± 0.007	0.0079 ± 0.0015	0.36 ± 0.53	0.0046
	Ni−Ni	12	2.956 ± 0.004	0.0075 ± 0.0003		
	Ni−O2	8	3.549 ± 0.026	0.0143 ± 0.0036		
1.20, C	Ni−O1	5.6 ± 0.4	2.070 ± 0.007	0.0074 ± 0.0014	0.22 ± 0.50	0.0043
	Ni−Ni	12	2.957 ± 0.004	0.0074 ± 0.0002		
	Ni−O2	8	3.547 ± 0.025	0.0143 ± 0.0035		

Table S4. Summary of the EXAFS best fit parameters for the prepared $Ni_{90}Fe_{10}O_y$ sample recorded at different electrode potentials. *Operando* X−ray absorption spectra were measured at the Ni K edge during a standard electrochemical OER polarization measurement. *N* denotes the coordination number of the given scattering path, *d* indicates the refined path length, σ^2 represents the Debye-Waller factor, ΔE_0 is the energy shift, and the R-factor represents the relative error of the fit and data. An amplitude reduction factor of S_0^2 = 0.94 was used. *k* was kept within the range of *k* = 2.6−12.5 $Å^{-1}$ and a fitting window of 3.4 Å in R-space was used in all cases. C is used to indicate the potential steps recorded during the cathodic scan.

E, V	Path	N	d, Å	σ^2, $Å^2$	E_0, eV	R-factor
1.20	Ni−O1	6.0 ± 0.4	2.076 ± 0.006	0.0062 ± 0.0012	-0.32 ± 0.50	0.0027
	Ni−Ni	12	2.956 ± 0.004	0.0068 ± 0.0002		
	Ni−O2	8	3.516 ± 0.023	0.0112 ± 0.0030		
1.30	Ni−O1	6.0 ± 0.4	2.076 ± 0.007	0.0061 ± 0.0013	-0.25 ± 0.53	0.0031
	Ni−Ni	12	2.956 ± 0.004	0.0068 ± 0.0003		
	Ni−O2	8	3.515 ± 0.025	0.0112 ± 0.0031		
1.40	Ni−O1	6.0 ± 0.4	2.076 ± 0.006	0.0062 ± 0.0012	-0.37 ± 0.51	0.0028
	Ni−Ni	12	2.956 ± 0.004	0.0068 ± 0.0002		
	Ni−O2	8	3.515 ± 0.024	0.0111 ± 0.0030		
1.45	Ni−O1	6.0 ± 0.4	2.075 ± 0.006	0.0062 ± 0.0012	-0.38 ± 0.52	0.0030
	Ni−Ni	12	2.956 ± 0.004	0.0068 ± 0.0002		
	Ni−O2	8	3.514 ± 0.024	0.0110 ± 0.0030		
1.50	Ni−O1	6.0 ± 0.4	2.076 ± 0.006	0.0061 ± 0.0012	-0.36 ± 0.51	0.0027
	Ni−Ni	12	2.956 ± 0.004	0.0067 ± 0.0002		
	Ni−O2	8	3.517 ± 0.024	0.0112 ± 0.0030		
1.60	Ni−O1	6.0 ± 0.4	2.076 ± 0.006	0.0061 ± 0.0012	-0.36 ± 0.51	0.0028
	Ni−Ni	12	2.956 ± 0.004	0.0068 ± 0.0002		
	Ni−O2	8	3.515 ± 0.024	0.0113 ± 0.0030		
1.65	Ni−O1	6.0 ± 0.4	2.075 ± 0.007	0.0061 ± 0.0013	-0.37 ± 0.53	0.0032
	Ni−Ni	12	2.956 ± 0.004	0.0069 ± 0.0003		
	Ni−O2	8	3.515 ± 0.025	0.0112 ± 0.0031		
1.20, C	Ni−O1	6.0 ± 0.4	2.076 ± 0.006	0.0061 ± 0.0012	-0.38 ± 0.51	0.0028
	Ni−Ni	12	2.956 ± 0.004	0.0068 ± 0.0002		
	Ni−O2	8	3.517 ± 0.024	0.0111 ± 0.0030		

Table S5. Summary of the EXAFS best fit parameters for the prepared $Ni_{70}Fe_{30}O_y$ sample recorded at different electrode potentials. *Operando* X−ray absorption spectra were measured at the Ni K edge during a standard electrochemical OER polarization measurement. *N* denotes the coordination number of the given scattering path, *d* indicates the refined path length, σ^2 represents the Debye-Waller factor, ΔE_0 is the energy shift, and the R-factor represents the relative error of the fit and data. An amplitude reduction factor of S_0^2 = 0.93 was used. *k* was kept within the range of *k* = 2.6−12.5 $Å^{-1}$ and a fitting window of 3.4 Å in R-space was used in all cases. C is used to indicate the potential steps recorded during the cathodic scan.

E, V	Path	N	d, Å	σ^2, $Å^2$	E_0, eV	R-factor
	Ni−O1	6.0 ± 0.4	2.070 ± 0.006	0.0069 ± 0.0011		
1.20	Ni−Ni	12	2.964 ± 0.004	0.0089 ± 0.0003	0.10 ± 0.49	0.0033
	Ni−O2	8	3.538 ± 0.025	0.0150 ± 0.0033		
	Ni−O1	5.8 ± 0.4	2.069 ± 0.006	0.0067 ± 0.0011		
1.40	Ni−Ni	12	2.963 ± 0.004	0.0089 ± 0.0003	0.12 ± 0.48	0.0033
	Ni−O2	8	3.534 ± 0.024	0.0145 ± 0.0031		
	Ni−O1	5.9 ± 0.4	2.069 ± 0.006	0.0068 ± 0.0011		
1.42	Ni−Ni	12	2.963 ± 0.004	0.0090 ± 0.0003	0.11 ± 0.50	0.0036
	Ni−O2	8	3.529 ± 0.025	0.0143 ± 0.0031		
	Ni−O1	5.9 ± 0.4	2.069 ± 0.006	0.0068 ± 0.0011		
1.44	Ni−Ni	12	2.963 ± 0.004	0.0091 ± 0.0003	0.10 ± 0.51	0.0036
	Ni−O2	8	3.526 ± 0.025	0.0142 ± 0.0032		
	Ni−O1	6.1 ± 0.4	2.068 ± 0.006	0.0071 ± 0.0011		
1.46	Ni−Ni	12	2.962 ± 0.004	0.0089 ± 0.0003	0.03 ± 0.51	0.0034
	Ni−O2	8	3.519 ± 0.024	0.0130 ± 0.0030		
	Ni−O1	6.0 ± 0.4	2.068 ± 0.005	0.0069 ± 0.0010		
1.50	Ni−Ni	12	2.964 ± 0.004	0.0088 ± 0.0002	0.12 ± 0.45	0.0027
	Ni−O2	8	3.528 ± 0.022	0.0140 ± 0.0028		
	Ni−O1	6.0 ± 0.4	2.068 ± 0.006	0.0069 ± 0.0011		
1.52	Ni−Ni	12	2.963 ± 0.004	0.0089 ± 0.0003	0.07 ± 0.48	0.0032
	Ni−O2	8	3.523 ± 0.023	0.0136 ± 0.0029		
	Ni−O1	6.1 ± 0.4	2.068 ± 0.006	0.0071 ± 0.0011		
1.54	Ni−Ni	12	2.963 ± 0.004	0.0090 ± 0.0003	0.01 ± 0.51	0.0035
	Ni−O2	8	3.520 ± 0.024	0.0134 ± 0.0031		
	Ni−O1	6.0 ± 0.4	2.069 ± 0.006	0.0070 ± 0.0011		
1.56	Ni−Ni	12	2.963 ± 0.004	0.0089 ± 0.0003	0.09 ± 0.48	0.0032
	Ni−O2	8	3.525 ± 0.023	0.0133 ± 0.0029		
	Ni−O1	6.0 ± 0.4	2.069 ± 0.006	0.0069 ± 0.0011		
1.58	Ni−Ni	12	2.964 ± 0.004	0.0090 ± 0.0003	0.12 ± 0.50	0.0034
	Ni−O2	8	3.524 ± 0.025	0.0140 ± 0.0031		
	Ni−O1	6.0 ± 0.4	2.068 ± 0.006	0.0069 ± 0.0011		
1.60	Ni−Ni	12	2.962 ± 0.004	0.0089 ± 0.0003	0.06 ± 0.48	0.0034
	Ni−O2	8	3.525 ± 0.023	0.0130 ± 0.0028		
	Ni−O1	6.0 ± 0.4	2.069 ± 0.006	0.0070 ± 0.0010		
1.20, C	Ni−Ni	12	2.963 ± 0.004	0.0088 ± 0.0002	0.13 ± 0.46	0.0028
	Ni−O2	8	3.527 ± 0.022	0.0135 ± 0.0028		